Research Paper

Construction and topological analysis of an endometriosis-related exosomal circRNA-miRNA-mRNA regulatory network

Jingni Wu[1], Xiaoling Fang[1], Hongyan Huang[1], Wei Huang[2,3], Lei Wang[4], Xiaomeng Xia[1]

[1]Department of Obstetrics and Gynecology, The Second Xiangya Hospital, Central South University, Changsha 410011, Hunan, China
[2]Research Center of Carcinogenesis and Targeted Therapy, Xiangya Hospital, Central South University, Changsha 410008, Hunan, China
[3]The Higher Educational Key Laboratory for Cancer Proteomics and Translational Medicine of Hunan Province, Xiangya Hospital, Central South University, Changsha 410008, Hunan, China
[4]NHC Key Laboratory of Carcinogenesis and the Key Laboratory of Carcinogenesis and Cancer Invasion of the Chinese Ministry of Education, Cancer Research Institute, School of Basic Medical Science, Central South University, Changsha 410078, Hunan, China

Correspondence to: Xiaomeng Xia; **email:** xiaxiaomeng@csu.edu.cn
Keywords: endometriosis, exosome, biomarker, circRNA, topological analysis
Received: September 29, 2020 **Accepted:** March 27, 2021 **Published:** April 26, 2021

ABSTRACT

Novel biomarkers are needed to accelerate the diagnosis and treatment of endometriosis. We performed RNA sequencing to explore the expression profiles of exosomal circular RNAs (circRNAs), microRNAs (miRNAs) and mRNAs in patients with ovarian endometriomas, eutopic endometria and normal endometria. Differentially expressed genes between the different pairs of groups were analyzed and functionally annotated. Then, miRNA-target RNA pairs were identified, competing endogenous RNA (ceRNA) scores were calculated, gene expression characteristics were determined, and these parameters were used to construct an exosomal ceRNA network. We identified 36 candidate hub genes with high degrees of gene connectivity. We also topologically analyzed the ceRNA network to obtain a hub ceRNA network of circRNAs with the highest closeness and ceRNA efficiency. Twelve genes overlapped between the 36 candidate hub genes and the genes in the hub ceRNA network. These 12 genes were considered to be exosomal RNA-based biomarkers, and circ_0026129/miRNA-15a-5p/ATPase H+ transporting V1 subunit A (*ATP6V1A*) were at the center of the ceRNA network. By determining the exosomal RNA expression profiles of endometriosis patients and constructing a circRNA-associated ceRNA network, these findings provide insight into the molecular pathways of endometriosis and new resources for its diagnosis and treatment.

INTRODUCTION

Endometriosis is a common, non-malignant gynecological disorder characterized by the growth of endometrial glands and stroma outside the uterus [1]. Up to 80% of women with chronic pelvic pain may have endometriosis, along with around 50% of women being treated for infertility [2, 3]. However, the pathogenesis of endometriosis is not well characterized, and there are often delays in diagnosing patients, leading to difficulties in medical and surgical treatments [4]. Therefore, it is essential to discover novel diagnostic biomarkers and therapeutic methods for endometriosis.

Noncoding RNAs such as circular RNAs (circRNAs) and microRNAs (miRNAs) are functional RNA molecules without protein-coding capacity. MiRNAs

can induce the degradation and inhibit the translation of their target mRNAs [5]. CircRNAs are covalently closed-loop structures generated from mRNAs through a splicing-like process (back-splicing). According to the competing endogenous RNA (ceRNA) theory, circRNAs can competitively bind to miRNAs as endogenous molecular sponges, ultimately altering mRNA expression. This circRNA regulatory mechanism indicates that there are communication networks among RNAs for regulating each other's expression via competing shared target miRNAs.

CeRNA networks involving circRNAs, miRNAs and mRNAs have been detected in many diseases, including cancer and Alzheimer's disease [6–8]. Systematic analysis of ceRNA network could significantly improve the functional understanding of coding and noncoding RNAs. In addition, changes in topologically important ceRNAs have been associated with the pathogenesis and treatment of lung adenocarcinoma, osteoarthritis, clear cell renal cell carcinoma and so on [9–11]. Hsa_circ_0067301 was identified as a ceRNA that suppresses Notch-1 expression by increasing miR-141 expression, and the downregulation of this circRNA was found to promote the epithelial-mesenchymal transition in endometriosis [12]. Topologically important hsa_circ_0002286/has-mir-222-5p/TRIM2 axis played a critical role in the progression of clear cell renal cell carcinoma [11]. However, there have been few studies of ceRNA networks in endometriosis.

Exosomes are a subset of extracellular vesicles that are critical for cellular communication [13]. They range in size from 30 to 150 nm, and transfer RNAs, lipids and proteins to recipient cells, thus participating in multiple diseases [14–16]. Exosomal RNAs are considered to be more functional than other RNAs because they are protected from RNase [17]. Therefore, exosomes may be a suitable setting for RNA crosstalk, and provide an ideal study model for the ceRNA hypothesis. Exosomal RNA biomarkers have been identified in various tumors [18, 19], and exosomes have been detected in all biological fluids [20], suggesting that exosomal RNAs could be used to diagnose and treat diseases [21, 22]. Exosomes secreted from endometriotic stromal cells can transfer information to other cells, contributing to the pathogenesis of endometriosis [23, 24]. However, little is known about the functions of exosomes or exosomal circRNA-miRNA-mRNA regulatory networks in endometriosis.

In this study, we derived exosomes from endometrial stromal cells, and used RNA sequencing to systematically analyze exosomal circRNA, miRNA and mRNA levels. Then, we constructed an exosomal ceRNA network, and topologically analyzed it to screen out hub RNAs for the construction of a hub ceRNA network. Finally, we identified the central genes in the ceRNA network, and used quantitative real-time PCR (qRT-PCR) to validate their expression in endometriosis. Our findings have clarified the molecular mechanisms of endometriosis and provided valuable information for its diagnosis and treatment.

RESULTS

Differentially expressed exosomal circRNAs, miRNAs and mRNAs in endometriosis

The flowchart of our work is shown in Figure 1. To identify differentially expressed exosomal circRNAs, miRNAs and mRNAs in endometriosis, we performed RNA sequencing on endometrial stromal cell-secreted exosomes from patients with ovarian endometriomas (EC), eutopic endometria (EU) and normal endometria (Ctrl). The top 10 differentially expressed circRNAs (DECs), miRNAs (DEMis) and mRNAs (DEMs) between the EC and Ctrl groups, between the EU and Ctrl groups, and between the EC and EU groups are shown as heatmaps (Supplementary Figure 1A–1C). The differences in circRNA expression between the respective pairs of groups are shown in Volcano plots (Figure 2A–2C).

Overlapping differentially expressed genes (DEGs) among the three comparison sets (EC vs. Ctrl, EU vs. Ctrl and EC vs. EU) were identified based on a log2 (fold-change) ≥ 1 and a corrected P-value < 0.001. Using these cutoff criteria, we identified 6512 overlapping circRNAs (2915 upregulated and 640 downregulated in all three comparison sets), 39 overlapping miRNAs (17 upregulated and 9 downregulated in all three comparison sets) and 1449 overlapping mRNAs (550 upregulated and 136 downregulated in all three comparison sets). These overlapping DEGs were used for subsequent analyses. Heatmaps of the overlapping DEGs revealed distinct RNA expression patterns in exosomes from EC, EU and Ctrl patients (Figure 2D–2F). Our results indicated that RNAs enriched in endometrial stromal cell-secreted exosomes may be involved in the etiology of endometriosis.

Functional enrichment analysis of DEMs

Next, we performed a gene set enrichment analysis (GSEA) to annotate the functions of the DEMs from the above pairwise comparisons. The top five enriched Kyoto Encyclopedia of Genes and Genomes (KEGG) pathways and the top five enriched Gene Ontology (GO) biological processes from the three comparisons are shown in Figure 3A–3C and

Supplementary Table 1. We also performed GO and KEGG pathway analyses on the overlapping DEMs from the three comparison sets (Figure 3D, 3E). The upregulated DEMs were mainly enriched in the 'epithelial to mesenchymal transition', 'positive regulation of endopeptidase activity', 'proteasome pathway' and 'Hippo signaling pathway' (Supplementary Table 2), while the downregulated DEMs were enriched in the 'negative regulation of insulin secretion involved in cellular response to glucose stimulus', 'positive regulation of cytokine production', 'metabolic pathway' and 'fatty acid degradation pathway' (Supplementary Table 3). These functions are known to be associated with endometriosis [25, 26], supporting our RNA sequencing analysis.

Prediction of miRNA-target interactions and ceRNA pairs

Subsequently, using the DEGs that overlapped among the three comparison sets (EC vs. Ctrl, EU vs. Ctrl and EC vs. EU), we determined the Pearson correlation coefficients between miRNAs and circRNAs/mRNAs, and used bioinformatic databases to predict miRNA-circRNA and miRNA-mRNA pairs. We then selected the overlapping miRNA-target pairs between the correlation analysis and the bioinformatic analysis. We obtained 1656 overlapping miRNA-circRNA pairs (including 25 miRNAs and 1154 circRNAs) from 29,441 miRNA-circRNA interactions ($R < -0.4$) and 12,206 miRNA-circRNA filtered target pairs (Figure 4A). In addition, we obtained 87 overlapping

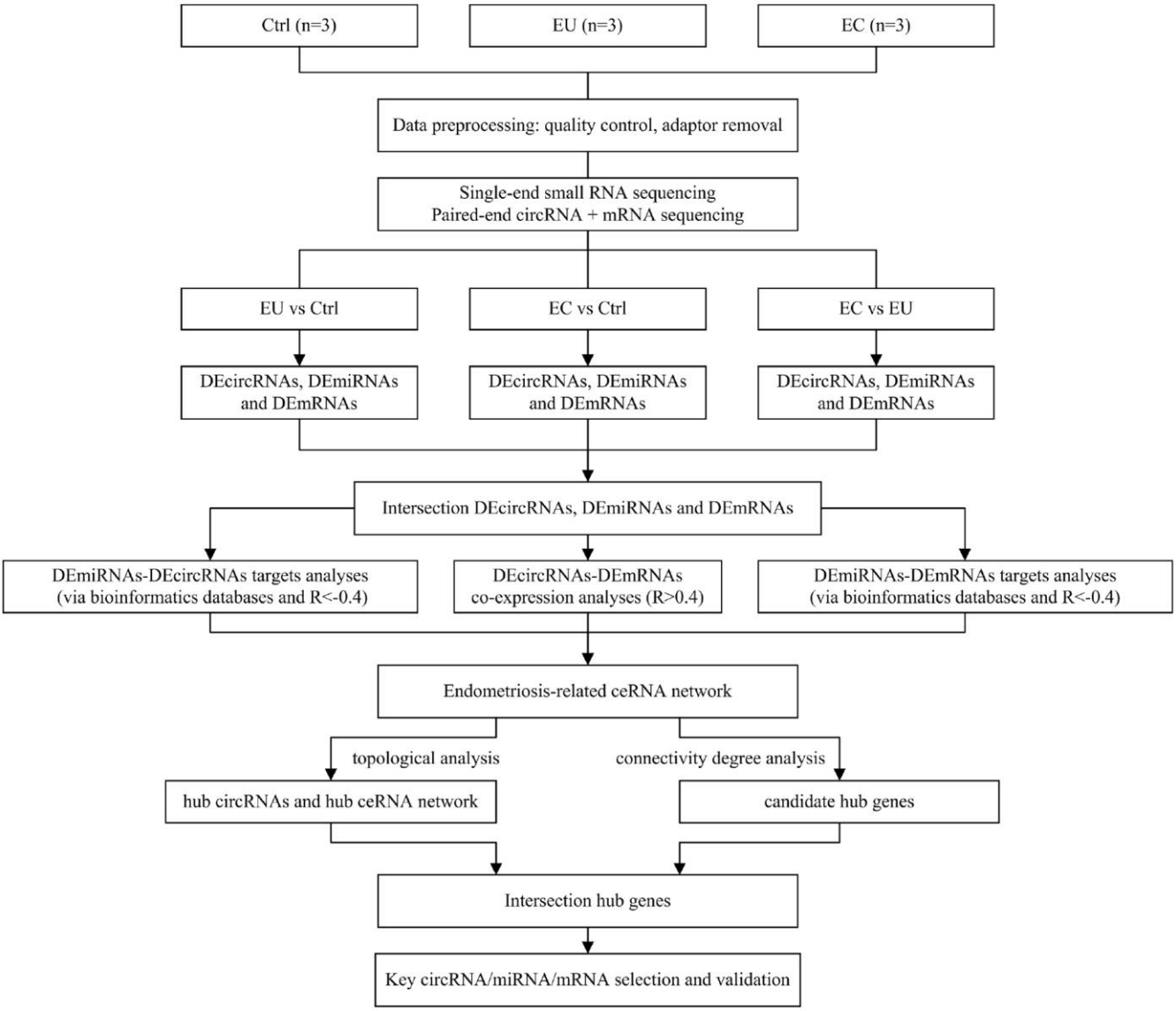

Figure 1. Flowchart of the data preparation, preprocessing and analysis strategy.

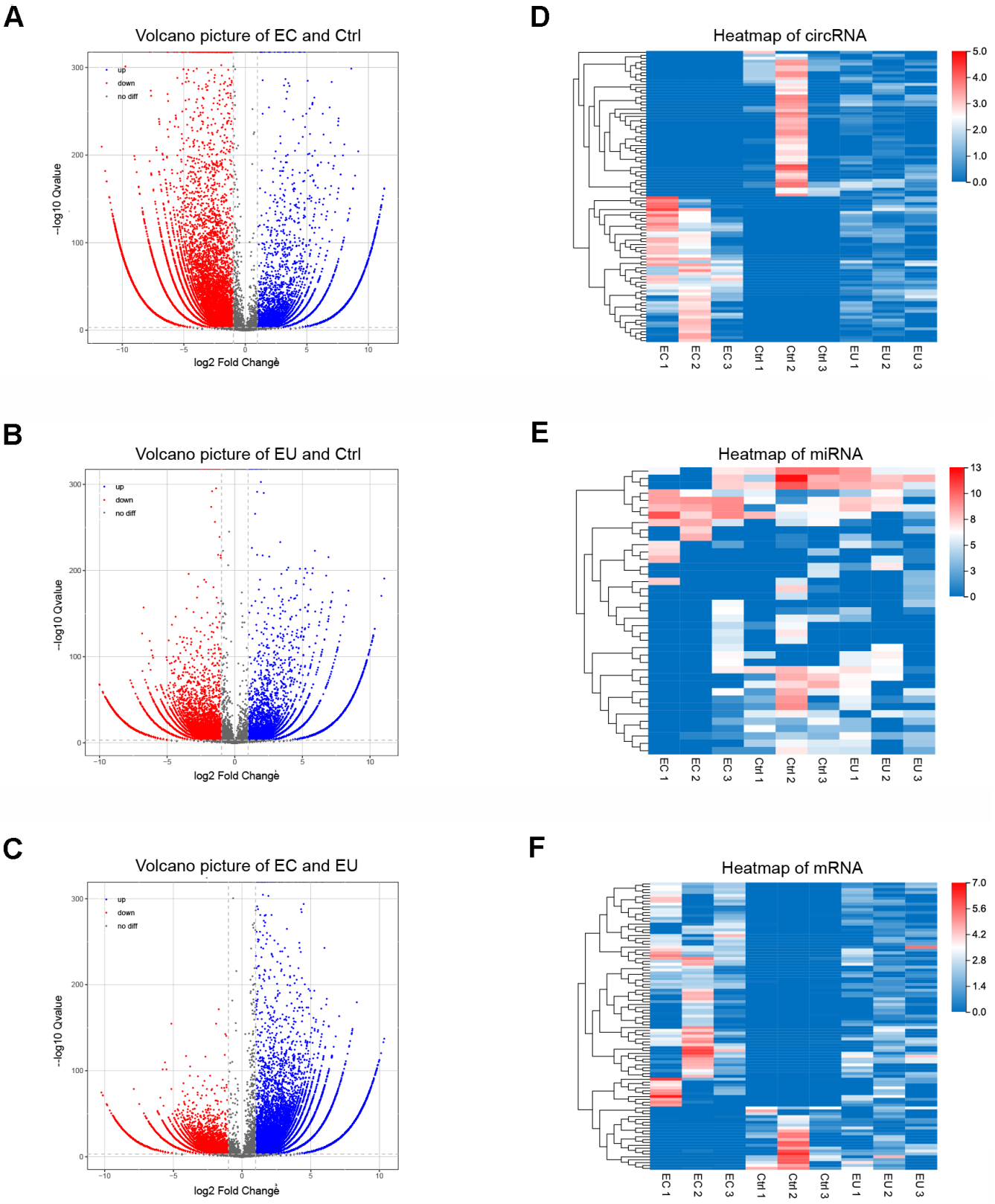

Figure 2. Identification of exosomal DECs, DEMis and DEMs in endometriosis. (**A**–**C**) Volcano plots of exosomal DECs based on the |log fold-change| between the EC and Ctrl groups (**A**), the EU and Ctrl groups (**B**) and the EC and EU groups (**C**). (**D**–**F**) Heatmap showing the expression of overlapping DEGs in the EC vs. Ctrl, EU vs. Ctrl and EC vs. EU comparisons, including the top 100 DECs, top 100 DEMis and top 100 DEMs. DECs, DEMis and DEMs: Differentially expressed circRNAs, miRNAs and mRNAs.

miRNA-mRNA pairs (including 25 miRNAs and 60 mRNAs) from 3894 miRNA-mRNA interactions (R < -0.4) and 1322 miRNA-mRNA filtered target pairs (Figure 4B).

Thereafter, we integrated these pairs based on shared miRNAs, and thus obtained 345,118 candidate circRNA-miRNA-mRNA competing interactions from the overlapping DEGs among the three comparison sets. When we filtered these competing interactions based on the circRNA-mRNA correlation (R > 0.4) and the ceRNA score (score > 0.3, P < 0.05), we identified 468 circRNA-mRNA ceRNA pairs (including 247 circRNAs and 23 mRNAs) (Figure 4C) and 10 shared miRNAs. The top 10 ceRNA pairs based on the ceRNA scores are shown in Table 1.

Construction of co-expression and ceRNA networks

We then constructed a co-expression network using the 468 ceRNA pairs identified above (Supplementary Figure 2), and established a ceRNA regulatory network using the 468 ceRNA pairs and 10 shared miRNAs (Figure 4D). The ceRNA network contained 247 circRNA nodes, 23 mRNA nodes, 10 miRNA nodes and 936 edges. It is well known that hub nodes with high

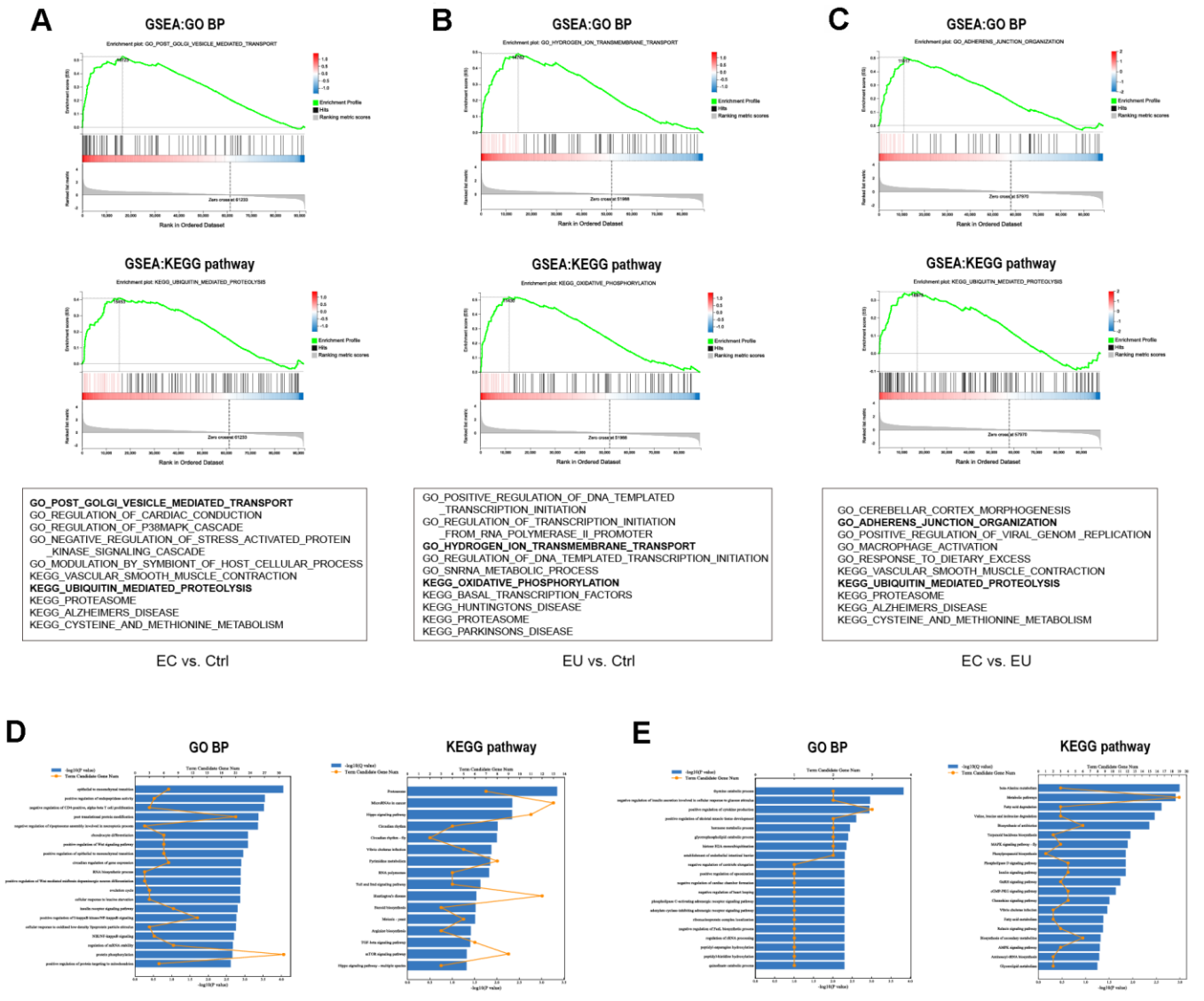

Figure 3. Functional enrichment analysis of DEMs. (**A**–**C**) The top 5 C5 GO biological processes and top 5 C2 KEGG pathways enriched in the DEMs between the EC and Ctrl groups (**A**), the EU and Ctrl groups (**B**) and the EC and EU groups (**C**) in the GSEA. The six most common functional gene sets in endometriosis are shown. (**D**, **E**) GO and KEGG pathway analyses of the overlapping upregulated DEMs (**D**) and downregulated DEMs (**E**) among the three comparison sets. GO: Gene ontology. BP: Biological process. KEGG: Kyoto Encyclopedia of Genes and Genomes.

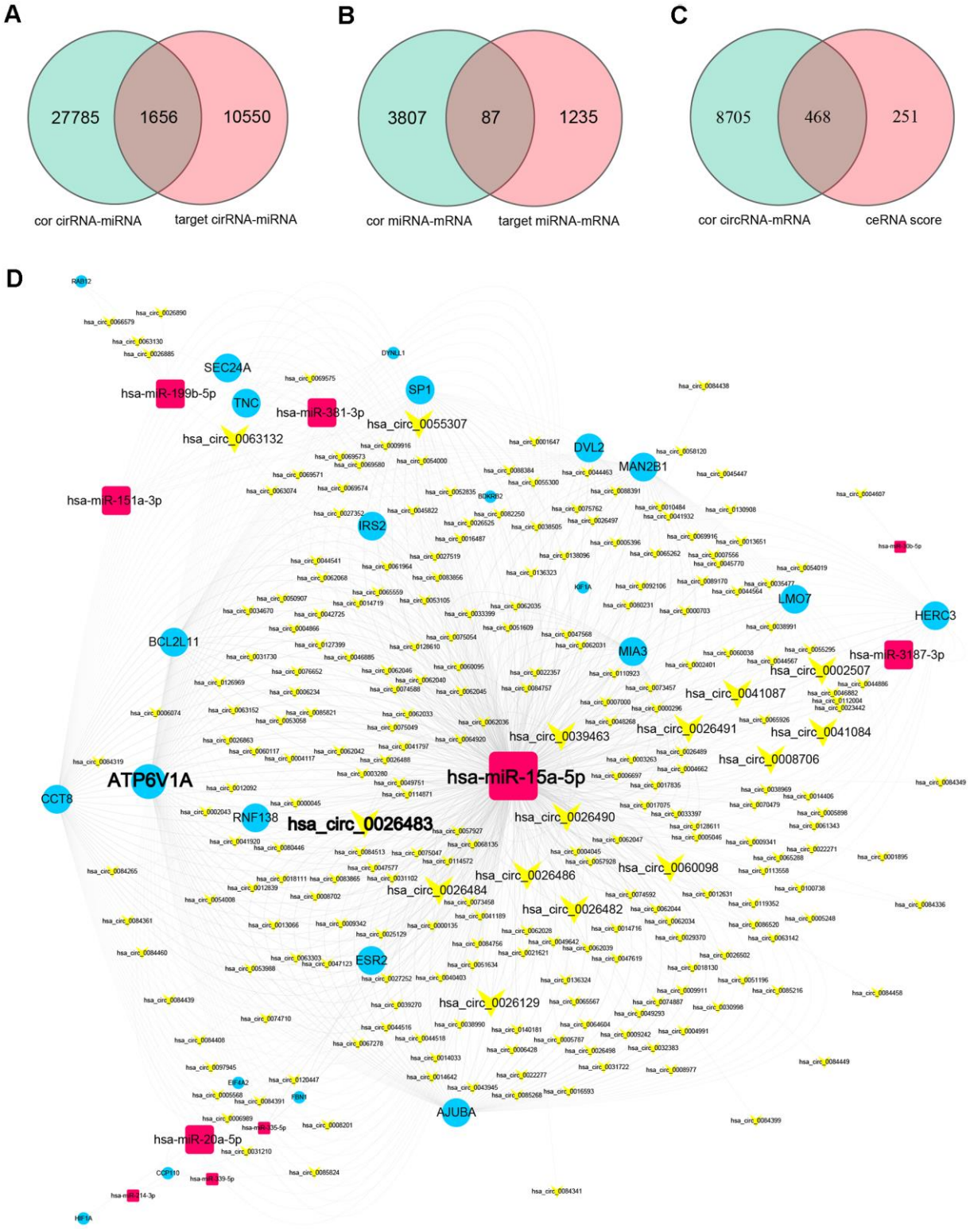

Figure 4. Prediction of miRNA-target interactions and ceRNA pairs, and construction of a circRNA-miRNA-mRNA ceRNA regulatory network. (**A**) MiRNA-circRNA interactions were filtered based on the miRNA-circRNA correlation coefficients and the miRNA-circRNA target pairs. (**B**) MiRNA-mRNA interactions were filtered based on the miRNA-mRNA correlation coefficients and the miRNA-mRNA target pairs. (**C**) Filtered miRNA-target interactions were integrated into circRNA-mRNA pairs (ceRNA pairs) based on shared miRNAs. CeRNA pairs were further filtered based on the ceRNA scores and the mRNA-circRNA correlation coefficients. (**D**) The ceRNA network. Yellow V-shaped nodes represent DECs, red rectangular nodes represent DEMis, and blue circular nodes represent DEMs. Larger nodes in the ceRNA network represent genes with higher degrees of connectivity.

Table 1. The top 10 ceRNA pairs based on the ceRNA score.

circRNA	mRNA	circ_m r	ceRNA Score	ceRNA P-value
hsa_circ_0026129	*ATP6V1A*	0.93917092	1	0.001059883
hsa_circ_0140181	*ATP6V1A*	0.823446797	1	0.001059883
hsa_circ_0026129	*MAN2B1*	0.802468977	1	0.001059883
hsa_circ_0014716	*DVL2*	0.831070515	1	0.001287001
hsa_circ_0110923	*DVL2*	0.695248588	1	0.001287001
hsa_circ_0080231	*HERC3*	0.516167256	1	0.00190779
hsa_circ_0048268	*CCT8*	0.936345086	1	0.002574003
hsa_circ_0000296	*CCT8*	0.913827698	1	0.002574003
hsa_circ_0026129	*RNF138*	0.620632147	1	0.00317965
hsa_circ_0014716	*LMO7*	0.729299492	1	0.004504505

ceRNA pair: circRNA-mRNA pair. circ_m r: the correlation coefficient between the circRNA and mRNA levels.

degrees of connectivity have vital functions in biological networks [27, 28]. Based on these studies and previous reports on genes associated with endometriosis, we identified 36 candidate hub nodes (degree ≥ 5) in the ceRNA network, including 15 circRNAs, 6 miRNAs and 15 mRNAs (Table 2 and Figure 4D).

Topological analysis and construction of a hub ceRNA sub-network

To construct a hub ceRNA sub-network, we analyzed the topological characteristics of the ceRNA network based on degree, closeness, ceRNA score and ceRNA P-value. Nine circRNAs overlapped among the top-ranking lists for these four characteristics, as shown in Figure 5A. We extracted the first miRNA neighbors and second mRNA neighbors of these hub circRNAs from the ceRNA network. Interestingly, these extracted mRNAs and miRNAs also had high degrees of connectivity and closeness. Hence, we used these genes to construct a hub ceRNA sub-network, which included 9 circRNA nodes, 3 miRNA nodes, 10 mRNA nodes and 66 edges (Figure 5C and Table 3).

Next, we determined which genes overlapped between the hub ceRNA sub-network and the list of 36 candidate hub genes with higher degrees of connectivity, assuming that these were the most important genes in the ceRNA network. We identified 12 overlapping hub genes, including 1 circRNA, 2 miRNAs and 9 mRNAs, which we selected as endometriosis-associated exosomal biomarkers (Figure 5B and Table 3). MiRNA-15a-5p and ATPase H+ transporting V1 subunit A (*ATP6V1A*) have previously been associated with endometriosis [29, 30], and exhibited high topological significance in our analysis. Circ_0026129 was the top-ranking target of miRNA-15a-5p, and exhibited high ceRNA efficiency. Hence, circ_0026129, miRNA-15a-5p and *ATP6V1A* were considered to be the center of the ceRNA network.

RT-PCR and miRNA target validation

We then used RT-PCR to validate the expression of circ_0026129, miRNA-15a-5p and *ATP6V1A* in stromal cell exosomes from the three groups of patients. The relative levels of these three RNAs estimated from the RT-PCR analysis are shown in Figure 6A–6C. The validation results were in agreement with the RNA sequencing results.

Finally, we used dual luciferase reporter assays to assess whether miRNA-15a-5p could bind directly to circ_0026129 and *ATP6V1A*. MiRNA-15a-5p mimics reduced the luciferase activities of reporter plasmids containing the potential binding sequences of wild-type circ_0026129 and *ATP6V1A*, but not of mutant circ_0026129 and *ATP6V1A* (Figure 6D, 6E). These results indicated that circ_0026129 may promote *ATP6V1A* expression by competing for miRNA-15a-5p in exosomes. This de-repression may enhance the release of ATP6V1A from endometrial stromal cells to recipient cells in the uterine or abdominal cavity, thus contributing to the pathogenesis of endometriosis.

DISCUSSION

Exosomes are crucial for both local and systemic cellular communication, due to their ability to transfer RNA between cells [13]. CircRNAs are endogenous noncoding RNAs with widespread distribution and various cellular functions [31, 32]. Recently, circRNAs have been reported to be enriched and stable in

Table 2. Differentially expressed genes with high degrees of connectivity (node degrees ≥ 5).

Number	Gene type	Gene name	Genbank description	Node degrees
1	miRNA	hsa-miR-15a-5p	NA	876
2	mRNA	*ATP6V1A*	ATPase H+ transporting V1 subunit A	87
3	mRNA	*CCT8*	Chaperonin containing TCP1 subunit 8	72
4	mRNA	*BCL2L11*	BCL2-like 11	66
5	mRNA	*AJUBA*	Ajuba LIM protein	45
6	mRNA	*MAN2B1*	Mannosidase alpha class 2B member 1	42
7	mRNA	*HERC3*	HECT and RLD domain containing E3 ubiquitin protein ligase 3	32
8	mRNA	*SP1*	Sp1 transcription factor	28
9	mRNA	*MIA3*	MIA SH3 domain ER export factor 3	21
10	mRNA	*DVL2*	Disheveled segment polarity protein 2	19
11	miRNA	hsa-miR-381-3p	NA	18
12	miRNA	hsa-miR-3187-3p	NA	12
13	mRNA	*RNF138*	Ring finger protein 138	10
14	circRNA	hsa_circ_0026129	NA	8
15	mRNA	*LMO7*	LIM domain 7	8
16	miRNA	hsa-miR-199b-5p	NA	8
17	circRNA	hsa_circ_0039463	NA	7
18	miRNA	hsa-miR-20a-5p	NA	6
19	circRNA	hsa_circ_0055307	NA	6
20	circRNA	hsa_circ_0041084	NA	6
21	circRNA	hsa_circ_0041087	NA	6
22	circRNA	hsa_circ_0002507	NA	6
23	circRNA	hsa_circ_0026483	NA	6
24	circRNA	hsa_circ_0008706	NA	6
25	circRNA	hsa_circ_0026490	NA	6
26	miRNA	hsa-miR-151a-3p	NA	6
27	mRNA	*SEC24A*	SEC24 homolog A, COPII coat complex component	6
28	circRNA	hsa_circ_0063132	NA	5
29	mRNA	*ESR2*	Estrogen receptor 2	5
30	circRNA	hsa_circ_0026486	NA	5
31	circRNA	hsa_circ_0060098	NA	5
32	mRNA	*IRS2*	Insulin receptor substrate 2	5
33	circRNA	hsa_circ_0026491	NA	5
34	circRNA	hsa_circ_0026484	NA	5
35	circRNA	hsa_circ_0026482	NA	5
36	mRNA	*TNC*	Tenascin C	5

exosomes [31, 33], although their involvement in endometriosis has not been demonstrated clearly. Endometriosis is a multifactorial disease, and ectopic implantation depends heavily on other pathological processes, including angiogenesis and immune dysfunction. Thus, exosomal ceRNAs could be important for the communication between endometrial stromal cells and other cells, such as vascular endothelial cells and immune cells.

To explore this possibility, we systematically analyzed exosomal RNA sequencing data, miRNA-target interactions and ceRNA co-expression data in endometriosis for the first time. Based on the ceRNA hypothesis, we constructed an exosomal circRNA-related ceRNA network, and then constructed a hub ceRNA sub-network based on closeness, degree and ceRNA scores. We identified 12 endometriosis-associated exosomal RNA biomarkers, and found that

circ_0026129, miRNA-15a-5p and *ATP6V1A* were at the center of the endometriosis-related exosomal ceRNA network. We used PCR to validate the expression of these three RNAs, and employed luciferase reporter assays to verify their molecular binding.

All the ceRNAs (i.e., circRNAs and mRNAs) in a ceRNA network should have three common characteristics [34]: (1) they should be differentially expressed between the comparison groups; (2) they should be the targets of miRNAs; and (3) their interrelationships should adhere to the competition rules

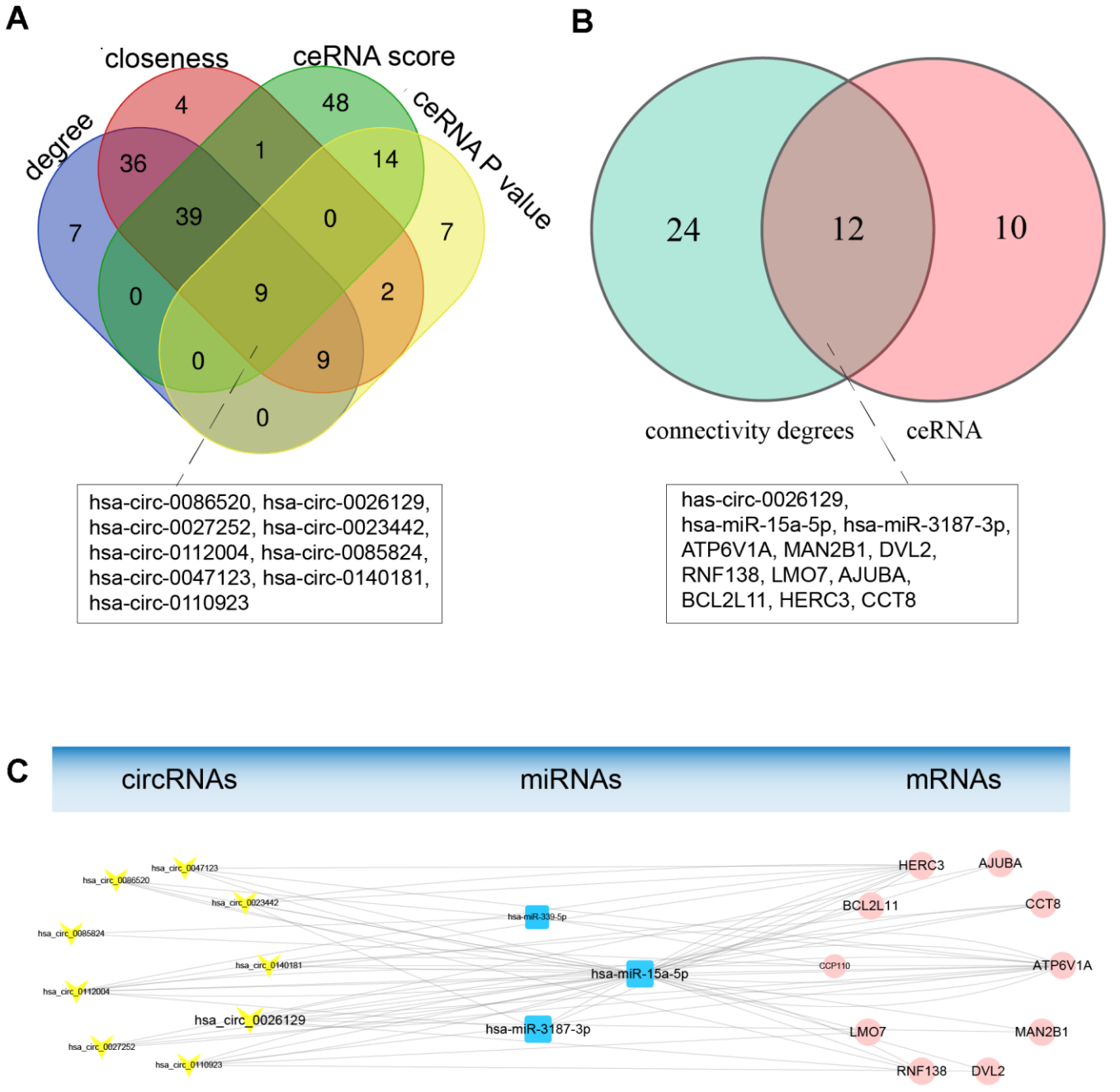

Figure 5. Topological analysis and construction of the hub ceRNA sub-network. (**A**) Topological characteristics of the ceRNA netwok. Nine hub circRNAs overlapped among the lists of genes with ceRNA scores > 0.7, genes with ceRNA P-values < 0.01 and the top 100 genes based on the degree of connectivity and betweenness. (**B**) Venn diagram of overlapping genes between the hub ceRNA network of nine circRNAs and the genes with higher degrees of connectivity. (**C**) The hub ceRNA sub-network containing the nine hub circRNAs. Yellow V-shaped nodes represent DECs, red rectangular nodes represent DEMis, and blue circular nodes represent DEMs. The larger nodes represent the overlapping hub genes.

Table 3. The topological characteristics of the hub ceRNA network.

circRNA	miRNA	mRNA	ceRNA score	ceRNA P-value	circRNA closeness	circRNA degree	miRNA closeness	miRNA degree	mRNA closeness	mRNA degree
hsa_circRNA_0023442	hsa-miR-15a-5p	*HERC3*	0.71429	0.00486	0.001739	2	0.003236	876	0.001751	32
hsa_circRNA_0023442	hsa-miR-3187-3p	*HERC3*	0.71429	0.00486	0.001739	2	0.001209	12	0.001751	32
hsa_circRNA_0026129	**hsa-miR-15a-5p**	***MAN2B1***	**1**	**0.00106**	**0.001733**	**8**	**0.003236**	**876**	**0.001733**	**42**
hsa_circRNA_0026129	**hsa-miR-15a-5p**	***ATP6V1A***	**1**	**0.00106**	**0.001733**	**8**	**0.003236**	**876**	**0.001733**	**87**
hsa_circRNA_0026129	**hsa-miR-15a-5p**	***RNF138***	**1**	**0.00318**	**0.001733**	**8**	**0.003236**	**876**	**0.001733**	**10**
hsa_circRNA_0026129	**hsa-miR-15a-5p**	***CCT8***	**0.75**	**0.00961**	**0.001733**	**8**	**0.003236**	**876**	**0.001733**	**72**
hsa_circRNA_0027252	hsa-miR-15a-5p	*AJUBA*	1	0.00721	0.001733	4	0.003236	876	0.001733	45
hsa_circRNA_0027252	hsa-miR-15a-5p	*ATP6V1A*	1	0.00721	0.001733	4	0.003236	876	0.001733	87
hsa_circRNA_0047123	hsa-miR-15a-5p	*ATP6V1A*	0.71429	0.00229	0.001733	3	0.003236	876	0.001733	87
hsa_circRNA_0047123	hsa-miR-15a-5p	*HERC3*	0.71429	0.00486	0.001733	3	0.003236	876	0.001751	32
hsa_circRNA_0085824	hsa-miR-339-5p	*CCP110*	0.75	0.00492	0.034483	1	0.047619	2	0.066667	4
hsa_circRNA_0086520	hsa-miR-15a-5p	*ATP6V1A*	0.71429	0.00229	0.001733	4	0.003236	876	0.001733	87
hsa_circRNA_0086520	hsa-miR-15a-5p	*RNF138*	0.71429	0.00915	0.001733	4	0.003236	876	0.001733	10
hsa_circRNA_0110923	hsa-miR-15a-5p	*DVL2*	1	0.00129	0.001733	3	0.003236	876	0.001733	19
hsa_circRNA_0110923	hsa-miR-15a-5p	*LMO7*	1	0.0045	0.001733	3	0.003236	876	0.001733	8
hsa_circRNA_0110923	hsa-miR-15a-5p	*ATP6V1A*	1	0.00721	0.001733	3	0.003236	876	0.001733	87
hsa_circRNA_0112004	hsa-miR-15a-5p	*BCL2L11*	0.8	0.00246	0.001739	4	0.003236	876	0.001733	66
hsa_circRNA_0112004	hsa-miR-15a-5p	*ATP6V1A*	0.8	0.00479	0.001739	4	0.003236	876	0.001733	87
hsa_circRNA_0112004	hsa-miR-15a-5p	*HERC3*	0.8	0.00838	0.001739	4	0.003236	876	0.001751	32
hsa_circRNA_0112004	hsa-miR-3187-3p	*HERC3*	0.8	0.00838	0.001739	4	0.001209	12	0.001751	32
hsa_circRNA_0140181	hsa-miR-15a-5p	*ATP6V1A*	1	0.00106	0.001733	3	0.003236	876	0.001733	87
hsa_circRNA_0140181	hsa-miR-15a-5p	*CCT8*	0.75	0.00961	0.001733	3	0.003236	876	0.001733	72

of the ceRNA network (for instance, that highly expressed circRNAs sequester miRNAs away from their target mRNAs, thus increasing mRNA expression). Competing RNAs with similar expression exhibit more robust ceRNA effects than ceRNA pairs that are largely differentially expressed [35]. The effectiveness of a ceRNA mainly depends on the number of sponged miRNAs [34], which can be reflected in the ceRNA score and ceRNA P-value.

Presently, there are many methods for ceRNA network construction, most of which only use RNA sequences to predict targets (as in the case of TargetScan) [36]. In our study, we constructed the ceRNA network not only by using bioinformatic tools to predict miRNA targets, but also by considering the competition among the circRNAs, miRNAs and mRNAs and removing interaction pairs with low ceRNA scores. To construct a hub ceRNA network, we identified hub genes with high

connectivity to other genes and high ceRNA effects. Circ_0026129, miRNA-15a-5p and *ATP6V1A* were at the center of the network and were differentially expressed between exosomes from endometriosis patients and controls, confirming the reliability of our RNA sequencing results.

Our results were consistent with previous reports. For example, *ATP6V1A* (one of the 12 most important genes identified in our study) has been associated with endometriosis severity and endometrial receptivity [29, 37], and is known to be an oncogene in endometrial cancer [38]. BCL2-like 11, a member of the BCL-2 family, is involved in apoptosis [39], and suppresses invasion in endometriosis by promoting the epithelial-mesenchymal transition [40]. MiRNA-15a-5p down-regulates vascular endothelial growth factor A, thus contributing to the pathogenesis of endometriosis [30, 41]. We also identified novel RNAs in endometriosis, such as *AJUBA* and miR-3187-3p. AJUBA is a negative regulator of the Hippo signaling pathway, which promotes cell proliferation and inhibits apoptosis in endometriosis [42, 43]. MiR-3187-3p was previously found to be involved in a ceRNA network that suppresses colorectal cancer cell proliferation [44]. There have been few studies about circRNAs in endometriosis, or about circ_0026129 in general. We found that circ_0026129 could bind to miRNA-15a-5p, which is known to be involved in endometriosis and correlated highly with endometriosis-related mRNAs.

To explore the underlying biological pathways of endometriosis, we performed a GSEA to identify the functions of the DEMs in each of the three comparison sets. Exosomal mRNAs from the EC, EU and Ctrl groups were enriched in different biological processes

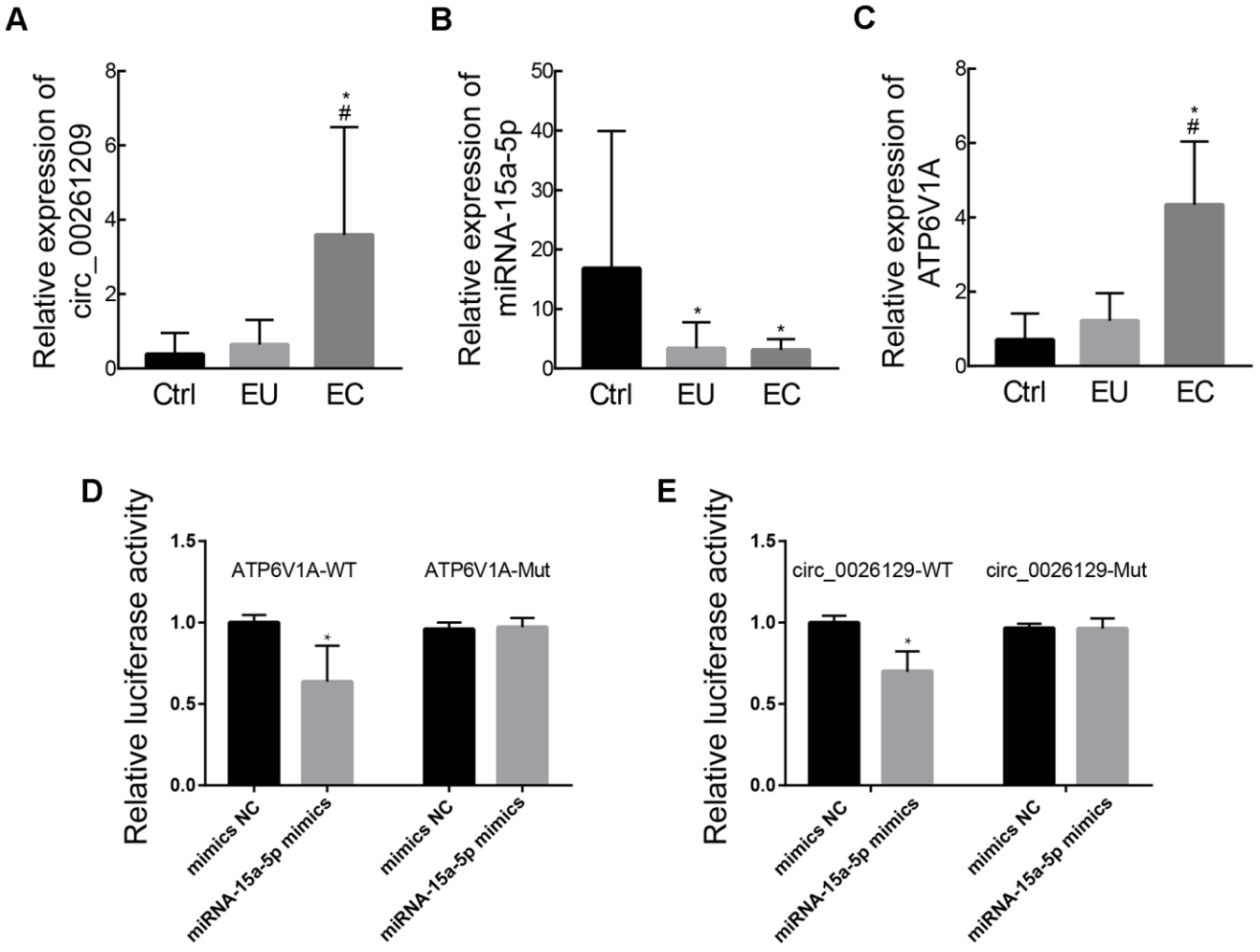

Figure 6. Validation of exosomal circ_0026129, miRNA-15a-5p and *ATP6V1A* expression and their molecular binding in endometriosis. (**A**–**C**) The relative expression of circ_0026129, miRNA-15a-5p and *ATP6V1A*, assessed using RT-PCR. (**D**, **E**) Luciferase reporter assay confirming that miRNA-15a-5p could bind to *ATP6V1A* and circ_0026129 in 293A cells.

and pathways, suggesting that exosome secretion uniquely contributes to the etiology of endometriosis. *ATP6V1A* was the core gene in the enriched GO 'hydrogen ion transmembrane transport' gene set and the KEGG 'oxidative phosphorylation' gene set. HECT and RLD domain containing E3 ubiquitin protein ligase 3 (*HERC3)* was the core gene in the enriched KEGG 'ubiquitin-mediated proteolysis' gene set in both the EC vs. Ctrl and EC vs. EU comparisons. Subsequently, we performed GO and KEGG enrichment analyses on the upregulated and downregulated exosomal DEMs that overlapped among the three comparison sets. The upregulated gene *ATP6V1A* was involved in 'mTOR signaling', an enriched KEGG pathway known to contribute to the development of endometriosis [45]. Our functional annotation suggested that the identified hub genes were strongly associated with endometriosis, and that the circ_0026129/miRNA-15a-5p/*ATP6V1A* ceRNA network may be important for the development of endometriosis.

To the best of our knowledge, this is the first study to identify a panel of endometriosis-related exosomal RNAs (circRNAs, miRNAs and mRNAs) and their competing relationships based on RNA sequencing data. This biomarker panel may be useful for diagnosing and evaluating the prognosis of endometriosis patients, but further experimental data are needed to delineate the mechanisms of the exosomal ceRNA network and confirm its relevance to the pathogenesis of endometriosis. Our sample size was relatively small. Nevertheless, our study had several strengths. Our RNA sequencing data were subjected to the RNA quality control procedures. Moreover, the DEGs we identified were involved in pathways that have been strongly associated with the development of endometriosis, such as the 'epithelial to mesenchymal transition' and the 'Hippo signaling pathway' [25, 43]. Additionally, the genes in the top-ranking interaction (circ_0026129/miRNA-15a-5p/*ATP6V1A*) were validated using RT-PCR. Our study has expanded the current understanding of RNA-RNA crosstalk in endometriosis, and our novel method of obtaining exosomal biomarkers has provided potential diagnostic and prognostic tools for this disorder.

MATERIALS AND METHODS

Ethics statement

Approval for our study was obtained from the Human Ethics Committee of Second Xiangya Hospital, Central South University. Each participant gave written informed consent in accordance with the Declaration of Helsinki.

Clinical specimens and cell culture

Primary endometrial stromal cells were obtained from thirteen ovarian endometriomas (EC) and thirteen eutopic endometria (EU) from women with histological diagnoses of stage III-IV endometriosis based on the American Society for Reproductive Medicine classification criteria, as well as from thirteen normal endometria from women who had undergone surgery due to tubal infertility without endometriosis (Ctrl). Three ovarian endometriomas, three eutopic endometria and three normal endometria were used for RNA sequencing, while the other samples were used for RT-PCR analysis. The endometrial tissues were pathologically confirmed in the proliferation stage. All patients were reproductive-age women with regular menstrual cycles, not taking any hormonal contraception or experiencing hormone-dependent disease during the past half year.

After being washed with phosphate-buffered saline, the collected tissues were minced and digested with 0.1% collagenase type I (Sigma-Aldrich, MO, USA) on a rocker for around 1 h (depending on the texture and cell type). Each specimen was centrifuged, and the sediment was cultured in Dulbecco's modified Eagle's medium (DMEM) with 10% fetal bovine serum (Thermo Fisher Scientific, MA, USA) in a 5% CO_2 incubator at 37° C. Immunohistochemical analysis of Vimentin indicated that endometrial stromal cells could be purified to 93-96% at passage 3. The purified endometrial stromal cells were used for exosome isolation.

Exosome isolation

When the cells were 70-80% confluent, the culture medium was replaced with serum-free DMEM for 48 h. Then, exosomes were extracted from the medium using an ExoQuick-TC exosome isolation kit (SBI, Palo Alto, CA, USA) in accordance with the manufacturer's protocol. In detail, the serum-free DMEM was collected and centrifuged for cell debris removal. Then, the supernatant was transferred to a sterile vessel, mixed with precipitation solution and incubated at 4° C overnight. On the second day, the mixture was centrifuged, the supernatant was discarded and the exosome pellet was isolated. The exosomes were stored in a -80° C freezer or used immediately for experiments.

Exosome validation

The exosomes were validated as previously described [46]. The exosomes were visualized using transmission electron microscopy. Paraformaldehyde (4%) was used to fix exosome fractions to carbon-coated electron

microscopy nickel grids. Each grid was further fixed with glutaraldehyde, stained with 0.5% aqueous uranyl acetate for 2 h and observed using transmission electron microscopy. Nanoparticle tracking analysis was used to determine the exosome distribution and concentration. Exosomes were diluted in phosphate-buffered saline and loaded into the test cell of a nanoparticle tracking instrument. Then, the nanoparticles were illuminated with a laser, and each sample was tracked automatically by the instrument based on Brownian motion. Additionally, the exosomal markers were analyzed using Western blotting.

RNA isolation, cDNA library preparation and RNA sequencing

Exosomal RNA sequencing was performed at the Beijing Genomics Institute (BGI, Shenzhen, China). In brief, total RNA was isolated from each exosome sample using Trizol reagent (Life Technologies, Gaithersburg, MD, USA). The quality and quantity of RNA were assessed with an Agilent 2100 Bioanalyzer (Thermo Fisher Scientific), and qRT-PCR was performed. rRNA depletion was performed on the total RNA.

Total RNA from each sample was used to construct a cDNA library. The sequencing libraries were sequenced on an Illumina HiSeq4000 or BGISEQ-500 platform in accordance with the manufacturer's recommendations. Paired-end reads were generated for miRNAs, whereas single-end reads were generated for circRNAs and mRNAs. Thereafter, low-quality reads and the adaptor sequences of the raw reads were discarded, and clean data were obtained and aligned using Bowtie2. Quality control procedures were used to ensure accurate measurements and correct acquirements. The mapped reads were further assembled using Cufflinks. DEMs, DEMis and DECs with statistical significance were identified using the DESeq package with the threshold of a fold-change > 2 and a corrected P-value < 0.001.

GO and KEGG pathway enrichment analyses of DEGs

In order to annotate the functions of the DEGs, we performed GO and KEGG enrichment analyses using 'phyper' [47], a hypergeometric distribution function in R. P-values < 0.05 were considered statistically significant.

GSEA

GSEA (http://www.broadinstitute.org/gsea/index.jsp) was performed on the EC, EU and Ctrl groups to investigate the biological functions and pathways involved in endometriosis. Java GSEA implementation was used for the analysis. The C2 (curated KEGG) and C5 (GO biological process) reference gene sets were obtained from the Molecular Signatures Database. Significant gene sets with P-values < 0.05 and false discovery rates < 25% were identified.

Prediction and refinement of miRNA-target interaction pairs

We first predicted miRNA-target interaction pairs using bioinformatic databases. MiRanda (http://miranda.org.uk), TargetScan (http://www.targetscan.org) and RNAhybrid-2.1.2 were used to predict miRNA-mRNA interactions. The StarBase database [48] was used to predict miRNA-circRNA interactions. MiRNA-mRNA and miRNA-circRNA pairs that overlapped with DEGs in the three comparison sets were selected.

We then predicted miRNA-target interaction pairs based on correlation coefficients. We evaluated the Pearson correlation coefficients between miRNA levels and circRNA/mRNA levels using the 'cor' function in R. Negative correlations between miRNAs and their targets (R < -0.4) were selected [34].

Finally, to enhance the reliability of prediction, we selected the overlapping miRNA–target interaction pairs between the bioinformatic analysis and the correlation coefficient analysis. Pairs that shared one miRNA were considered as candidate circRNA-miRNA-mRNA interactions for the subsequent ceRNA prediction.

Prediction and refinement of ceRNA pairs

We first predicted ceRNA pairs by evaluating the Pearson correlation coefficients between circRNA and mRNA levels. Positive correlations between circRNAs and mRNAs (R > 0.4) were selected. We chose ceRNA (circRNA-mRNA) pairs based on these co-expression values and circRNA-miRNA-mRNA competing interactions.

We then predicted ceRNA pairs by computing ceRNA scores [35]. The ceRNA score was calculated as the number of shared miRNAs between a ceRNA pair (circRNA-mRNA) divided by the total number of miRNAs targeting the individual candidate genes [35]. The P-value for each potential ceRNA pair was determined using a hypergeometric test based on the previously described formula $P = \sum_{i=c}^{\min(K,n)} \binom{K}{i}\binom{N-K}{n-i} \Big/ \binom{N}{n}$, where K is the

number of miRNAs interacting with a specified gene, n is the number of miRNAs interacting with the ceRNA of the specified gene, c is the number of shared miRNAs between these two genes, and N is the total number of miRNAs [28]. CeRNA pairs with corrected P-values > 0.05 or ceRNA scores ≤ 0.3 were removed.

Finally, we refined the ceRNA pairs based on both their Pearson correlation coefficients and their ceRNA scores.

Construction of co-expression and ceRNA networks

CeRNA pairs were used to construct a circRNA-mRNA co-expression network. Then, a circRNA-miRNA-mRNA ceRNA network was constructed based on the ceRNA pairs that shared miRNAs. Genes with high degrees of connectivity tended to be at the center of the ceRNA network, so we calculated the degrees of connectivity for nodes in the ceRNA network. Cytoscape was used to visualize the ceRNA network. Larger nodes were used to represent genes with higher degrees of connectivity.

Topological analysis and construction of the hub ceRNA sub-network

A topological analysis of circRNAs in the ceRNA network was conducted to identify the hub nodes of endometriosis. Topological parameters (the ceRNA score, ceRNA P-value, degree, and closeness) were calculated using the Cytoscape plug-in CentiScaPe. The top-ranking circRNAs for these four topological parameters were compared, and those that overlapped were used to construct a hub ceRNA sub-network. A Venn diagram was used to identify genes that overlapped between the hub ceRNA sub-network and the list of genes with higher degrees of connectivity. Cytoscape was used to visualize the sub-network. Larger nodes were used to represent overlapping hub genes.

Reverse transcription and polymerase chain reaction (RT-PCR) analysis

To validate the RNA sequencing data, we performed RT-PCR on stromal cell exosomes from the EC (n=10), EU (n=10), and Ctrl (n=10) groups. A miRNA/HiFiScript cDNA Synthesis Kit (CWBio Co. Ltd., Beijing, China) was used to reverse-transcribe total RNA into first-strand cDNA. Ultra SYBR Mixture (Low ROX) (CWBio Co. Ltd.) was used to amplify the cDNA samples. The primers are listed in Supplementary Table 4. U6 was used as an internal control for miRNAs, while *β-actin* was used as an internal control for circRNAs and mRNAs [49]. The primers were designed using primer5. Candidate circRNAs were characterized by RT-PCR using the outward-facing primers annealing at the distal ends of the circRNAs [50, 51]. The sequence specificity was verified through BLAST searches. The mean Ct value of all the technical replicates for each sample was assessed, and relative RNA expression was calculated using the $2^{-\Delta\Delta Ct}$ method.

Luciferase reporter assay

Reporter plasmids expressing wild-type (WT) and mutant (MUT) sequences for the 3′ untranslated regions (3′UTRs) of circ_0026129 (pHG-MirTarget-circ_0026129-3′UTR-WT and pHG-MirTarget-circ_0026129-3′UTR-MUT, respectively) and *ATP6V1A* (pHG-MirTarget-ATP6V1A-3′UTR-WT and pHG-MirTarget-ATP6V1A-3′UTR-MUT, respectively) were obtained from HonorGene Biotechnology, along with miRNA-15a-5p mimics and negative control (miRNA-15a-5p-NC) plasmids. To confirm that miRNA-15a-5p could bind directly to the 3′UTRs of circ_0026129 and *ATP6V1A*, we co-transfected 293A cells with the pHG-MirTarget-circ_0026129-3′UTR-WT, pHG-MirTarget-circ_0026129-3′UTR-MUT, pHG-MirTarget-ATP6V1A-3′UTR-WT or pHG-MirTarget-ATP6V1A-3′UTR-MUT reporter plasmids and either miRNA-15a-5p mimics or miRNA-15a-5p-NC. Twenty-four hours after transfection, luciferase activity was measured on a Dual-Luciferase Reporter Assay System (Promega, Madison, WI, USA). The ratio of luciferase activity was calculated for each sample, in accordance with the manufacturer's instructions.

Statistical analysis

The data presented in our study are representative of three independent experiments. The results were analyzed using one-way analysis of variance with Fisher's least significant difference post hoc test in SPSS version 23 (SPSS Inc., Chicago, IL, USA). Data are presented as the mean ± standard deviation. P-values < 0.05 were considered statistically significant.

Data availability

The data that support the findings of this study are available from the corresponding author upon reasonable request.

AUTHOR CONTRIBUTIONS

J.W. and X.X. conceived and designed the experiments. J.W., X.F., H.H. and W.H. performed the experiments and acquired the data. J.W., H.H. and L.W. analyzed the data. J.W. drafted and critically evaluated the article.

ACKNOWLEDGMENTS

The authors are thankful to Yizhou Wang at the AGCT Core of Cedar-Sinai Medical Center for helpful discussions of the manuscript.

CONFLICTS OF INTEREST

The authors declare that the research was conducted in the absence of any commercial or financial relationships that could be construed as a potential conflict of interest.

FUNDING

This work was supported by the National Natural Science Foundation of China (grant numbers 81671437, 81771558 and 81702924), the Natural Science Foundation of Hunan Province (grant number 2020JJ4814) and the Fundamental Research Funds for the Central Universities of Central South University (grant number 2020zzts285). The authors have no relevant affiliations or financial involvement with any organization or entity with a financial interest in or financial conflict with the subject matter or materials discussed in the manuscript apart from those disclosed.

REFERENCES

1. Giudice LC, Kao LC. Endometriosis. Lancet. 2004; 364:1789–99. https://doi.org/10.1016/S0140-6736(04)17403-5 PMID:15541453

2. Słabuszewska-Jóźwiak A, Ciebiera M, Baran A, Jakiel G. Effectiveness of laparoscopic surgeries in treating infertility related to endometriosis. Ann Agric Environ Med. 2015; 22:329–31. https://doi.org/10.5604/12321966.1152089 PMID:26094533

3. Wu D, Lu P, Mi X, Miao J. Exosomal miR-214 from endometrial stromal cells inhibits endometriosis fibrosis. Mol Hum Reprod. 2018; 24:357–65. https://doi.org/10.1093/molehr/gay019 PMID:29660008

4. Bedaiwy MA, Alfaraj S, Yong P, Casper R. New developments in the medical treatment of endometriosis. Fertil Steril. 2017; 107:555–65. https://doi.org/10.1016/j.fertnstert.2016.12.025 PMID:28139238

5. Beermann J, Piccoli MT, Viereck J, Thum T. Non-coding RNAs in Development and Disease: Background, Mechanisms, and Therapeutic Approaches. Physiol Rev. 2016; 96:1297–325. https://doi.org/10.1152/physrev.00041.2015 PMID:27535639

6. Xiong DD, Dang YW, Lin P, Wen DY, He RQ, Luo DZ, Feng ZB, Chen G. A circRNA-miRNA-mRNA network identification for exploring underlying pathogenesis and therapy strategy of hepatocellular carcinoma. J Transl Med. 2018; 16:220. https://doi.org/10.1186/s12967-018-1593-5 PMID:30092792

7. Guan YJ, Ma JY, Song W. Identification of circRNA-miRNA-mRNA regulatory network in gastric cancer by analysis of microarray data. Cancer Cell Int. 2019; 19:183. https://doi.org/10.1186/s12935-019-0905-z PMID:31346318

8. Ma N, Pan J, Ye X, Yu B, Zhang W, Wan J. Whole-Transcriptome Analysis of APP/PS1 Mouse Brain and Identification of circRNA-miRNA-mRNA Networks to Investigate AD Pathogenesis. Mol Ther Nucleic Acids. 2019; 18:1049–62. https://doi.org/10.1016/j.omtn.2019.10.030 PMID:31786335

9. Song W, Fu T. Circular RNA-Associated Competing Endogenous RNA Network and Prognostic Nomogram for Patients With Colorectal Cancer. Front Oncol. 2019; 9:1181. https://doi.org/10.3389/fonc.2019.01181 PMID:31781492

10. Zhou ZB, Huang GX, Fu Q, Han B, Lu JJ, Chen AM, Zhu L. circRNA.33186 Contributes to the Pathogenesis of Osteoarthritis by Sponging miR-127-5p. Mol Ther. 2019; 27:531–41. https://doi.org/10.1016/j.ymthe.2019.01.006 PMID:30692016

11. Wei X, Dong Y, Chen X, Ren X, Li G, Wang Y, Wang Y, Zhang T, Wang S, Qin C, Song N. Construction of circRNA-based ceRNA network to reveal the role of circRNAs in the progression and prognosis of metastatic clear cell renal cell carcinoma. Aging (Albany NY). 2020; 12:24184–207. https://doi.org/10.18632/aging.104107 PMID:33223511

12. Zhang M, Wang S, Tang L, Wang X, Zhang T, Xia X, Fang X. Downregulated circular RNA hsa_circ_0067301 regulates epithelial-mesenchymal transition in endometriosis via the miR-141/Notch signaling pathway. Biochem Biophys Res Commun. 2019; 514:71–77. https://doi.org/10.1016/j.bbrc.2019.04.109 PMID:31023528

13. Milane L, Singh A, Mattheolabakis G, Suresh M, Amiji MM. Exosome mediated communication within the

tumor microenvironment. J Control Release. 2015; 219:278–94. https://doi.org/10.1016/j.jconrel.2015.06.029 PMID:26143224

14. Pérez-Boza J, Pegtel DM. Exosomes take (germinal) center stage. EMBO Rep. 2020; 21:e50190. https://doi.org/10.15252/embr.202050190 PMID:32147923

15. Zhang W, Jiang X, Bao J, Wang Y, Liu H, Tang L. Exosomes in Pathogen Infections: A Bridge to Deliver Molecules and Link Functions. Front Immunol. 2018; 9:90. https://doi.org/10.3389/fimmu.2018.00090 PMID:29483904

16. Sun Z, Yang S, Zhou Q, Wang G, Song J, Li Z, Zhang Z, Xu J, Xia K, Chang Y, Liu J, Yuan W. Emerging role of exosome-derived long non-coding RNAs in tumor microenvironment. Mol Cancer. 2018; 17:82. https://doi.org/10.1186/s12943-018-0831-z PMID:29678180

17. Dragomir M, Chen B, Calin GA. Exosomal lncRNAs as new players in cell-to-cell communication. Transl Cancer Res. 2018 (Suppl 2); 7:S243–52. https://doi.org/10.21037/tcr.2017.10.46 PMID:30148073

18. Ge Y, Mu W, Ba Q, Li J, Jiang Y, Xia Q, Wang H. Hepatocellular carcinoma-derived exosomes in organotropic metastasis, recurrence and early diagnosis application. Cancer Lett. 2020; 477:41–48. https://doi.org/10.1016/j.canlet.2020.02.003 PMID:32112905

19. Dai D, Tan Y, Guo L, Tang A, Zhao Y. Identification of exosomal miRNA biomarkers for diagnosis of papillary thyroid cancer by small RNA sequencing. Eur J Endocrinol. 2020; 182:111–21. https://doi.org/10.1530/EJE-19-0524 PMID:31721725

20. Kalluri R, LeBleu VS. Discovery of Double-Stranded Genomic DNA in Circulating Exosomes. Cold Spring Harb Symp Quant Biol. 2016; 81:275–80. https://doi.org/10.1101/sqb.2016.81.030932 PMID:28424339

21. Krause M, Samoylenko A, Vainio SJ. Exosomes as renal inductive signals in health and disease, and their application as diagnostic markers and therapeutic agents. Front Cell Dev Biol. 2015; 3:65. https://doi.org/10.3389/fcell.2015.00065 PMID:26539435

22. Aghebati-Maleki A, Nami S, Baghbanzadeh A, Karzar BH, Noorolyai S, Fotouhi A, Aghebati-Maleki L. Implications of exosomes as diagnostic and therapeutic strategies in cancer. J Cell Physiol. 2019; 234:21694–706. https://doi.org/10.1002/jcp.28875 PMID:31161617

23. Sun H, Li D, Yuan M, Li Q, Zhen Q, Li N, Wang G. Macrophages alternatively activated by endometriosis-exosomes contribute to the development of lesions in mice. Mol Hum Reprod. 2019; 25:5–16. https://doi.org/10.1093/molehr/gay049 PMID:30428082

24. Harp D, Driss A, Mehrabi S, Chowdhury I, Xu W, Liu D, Garcia-Barrio M, Taylor RN, Gold B, Jefferson S, Sidell N, Thompson W. Exosomes derived from endometriotic stromal cells have enhanced angiogenic effects *in vitro*. Cell Tissue Res. 2016; 365:187–96. https://doi.org/10.1007/s00441-016-2358-1 PMID:26841879

25. Zondervan KT, Becker CM, Koga K, Missmer SA, Taylor RN, Viganò P. Endometriosis. Nat Rev Dis Primers. 2018; 4:9. https://doi.org/10.1038/s41572-018-0008-5 PMID:30026507

26. Zhou WJ, Yang HL, Shao J, Mei J, Chang KK, Zhu R, Li MQ. Anti-inflammatory cytokines in endometriosis. Cell Mol Life Sci. 2019; 76:2111–32. https://doi.org/10.1007/s00018-019-03056-x PMID:30826860

27. Han JD, Bertin N, Hao T, Goldberg DS, Berriz GF, Zhang LV, Dupuy D, Walhout AJ, Cusick ME, Roth FP, Vidal M. Evidence for dynamically organized modularity in the yeast protein-protein interaction network. Nature. 2004; 430:88–93. https://doi.org/10.1038/nature02555 PMID:15190252

28. Wang Q, Cai J, Fang C, Yang C, Zhou J, Tan Y, Wang Y, Li Y, Meng X, Zhao K, Yi K, Zhang S, Zhang J, et al. Mesenchymal glioblastoma constitutes a major ceRNA signature in the TGF-β pathway. Theranostics. 2018; 8:4733–49. https://doi.org/10.7150/thno.26550 PMID:30279734

29. Aghajanova L, Giudice LC. Molecular evidence for differences in endometrium in severe versus mild endometriosis. Reprod Sci. 2011; 18:229–51. https://doi.org/10.1177/1933719110386241 PMID:21063030

30. Liu XJ, Bai XG, Teng YL, Song L, Lu N, Yang RQ. miRNA-15a-5p regulates VEGFA in endometrial mesenchymal stem cells and contributes to the pathogenesis of endometriosis. Eur Rev Med Pharmacol Sci. 2016; 20:3319–26. PMID:27608888

31. Wang Y, Liu J, Ma J, Sun T, Zhou Q, Wang W, Wang G, Wu P, Wang H, Jiang L, Yuan W, Sun Z, Ming L. Exosomal circRNAs: biogenesis, effect and application in human diseases. Mol Cancer. 2019; 18:116.

https://doi.org/10.1186/s12943-019-1041-z PMID:31277663

32. Lei M, Zheng G, Ning Q, Zheng J, Dong D. Translation and functional roles of circular RNAs in human cancer. Mol Cancer. 2020; 19:30. https://doi.org/10.1186/s12943-020-1135-7 PMID:32059672

33. Sun J, Li B, Shu C, Ma Q, Wang J. Functions and clinical significance of circular RNAs in glioma. Mol Cancer. 2020; 19:34. https://doi.org/10.1186/s12943-019-1121-0 PMID:32061256

34. Salmena L, Poliseno L, Tay Y, Kats L, Pandolfi PP. A ceRNA hypothesis: the Rosetta Stone of a hidden RNA language? Cell. 2011; 146:353–58. https://doi.org/10.1016/j.cell.2011.07.014 PMID:21802130

35. Ala U, Karreth FA, Bosia C, Pagnani A, Taulli R, Léopold V, Tay Y, Provero P, Zecchina R, Pandolfi PP. Integrated transcriptional and competitive endogenous RNA networks are cross-regulated in permissive molecular environments. Proc Natl Acad Sci USA. 2013; 110:7154–59. https://doi.org/10.1073/pnas.1222509110 PMID:23536298

36. Agarwal V, Bell GW, Nam JW, Bartel DP. Predicting effective microRNA target sites in mammalian mRNAs. Elife. 2015; 4:e05005. https://doi.org/10.7554/eLife.05005 PMID:26267216

37. Díaz-Gimeno P, Horcajadas JA, Martínez-Conejero JA, Esteban FJ, Alamá P, Pellicer A, Simón C. A genomic diagnostic tool for human endometrial receptivity based on the transcriptomic signature. Fertil Steril. 2011; 95:50–60, 60.e1–15. https://doi.org/10.1016/j.fertnstert.2010.04.063 PMID:20619403

38. Shivakumar M, Miller JE, Dasari VR, Gogoi R, Kim D. Exome-Wide Rare Variant Analysis From the DiscovEHR Study Identifies Novel Candidate Predisposition Genes for Endometrial Cancer. Front Oncol. 2019; 9:574. https://doi.org/10.3389/fonc.2019.00574 PMID:31338326

39. Concannon CG, Tuffy LP, Weisová P, Bonner HP, Dávila D, Bonner C, Devocelle MC, Strasser A, Ward MW, Prehn JH. AMP kinase-mediated activation of the BH3-only protein Bim couples energy depletion to stress-induced apoptosis. J Cell Biol. 2010; 189:83–94. https://doi.org/10.1083/jcb.200909166 PMID:20351066

40. Wang H, Sha L, Huang L, Yang S, Zhou Q, Luo X, Shi B. LINC00261 functions as a competing endogenous RNA to regulate BCL2L11 expression by sponging miR-132-3p in endometriosis. Am J Transl Res. 2019; 11:2269–79. PMID:31105834

41. Nothnick WB. MicroRNAs and Endometriosis: Distinguishing Drivers from Passengers in Disease Pathogenesis. Semin Reprod Med. 2017; 35:173–80. https://doi.org/10.1055/s-0037-1599089 PMID:28212593

42. Das Thakur M, Feng Y, Jagannathan R, Seppa MJ, Skeath JB, Longmore GD. Ajuba LIM proteins are negative regulators of the Hippo signaling pathway. Curr Biol. 2010; 20:657–62. https://doi.org/10.1016/j.cub.2010.02.035 PMID:20303269

43. Song Y, Fu J, Zhou M, Xiao L, Feng X, Chen H, Huang W. Activated Hippo/Yes-Associated Protein Pathway Promotes Cell Proliferation and Anti-apoptosis in Endometrial Stromal Cells of Endometriosis. J Clin Endocrinol Metab. 2016; 101:1552–61. https://doi.org/10.1210/jc.2016-1120 PMID:26977530

44. Yang G, Zhang T, Ye J, Yang J, Chen C, Cai S, Ma J. Circ-ITGA7 sponges miR-3187-3p to upregulate ASXL1, suppressing colorectal cancer proliferation. Cancer Manag Res. 2019; 11:6499–509. https://doi.org/10.2147/CMAR.S203137 PMID:31372051

45. Barra F, Ferro Desideri L, Ferrero S. Inhibition of PI3K/AKT/mTOR pathway for the treatment of endometriosis. Br J Pharmacol. 2018; 175:3626–27. https://doi.org/10.1111/bph.14391 PMID:29984446

46. Wu J, Huang H, Huang W, Wang L, Xia X, Fang X. Analysis of exosomal lncRNA, miRNA and mRNA expression profiles and ceRNA network construction in endometriosis. Epigenomics. 2020; 12:1193–213. https://doi.org/10.2217/epi-2020-0084 PMID:32462942

47. Chavez L, Jozefczuk J, Grimm C, Dietrich J, Timmermann B, Lehrach H, Herwig R, Adjaye J. Computational analysis of genome-wide DNA methylation during the differentiation of human embryonic stem cells along the endodermal lineage. Genome Res. 2010; 20:1441–50. https://doi.org/10.1101/gr.110114.110 PMID:20802089

48. Yang JH, Li JH, Shao P, Zhou H, Chen YQ, Qu LH. starBase: a database for exploring microRNA-mRNA interaction maps from Argonaute CLIP-Seq and Degradome-Seq data. Nucleic Acids Res. 2011; 39:D202–09. https://doi.org/10.1093/nar/gkq1056 PMID:21037263

49. Ou R, Lv M, Liu X, Lv J, Zhao J, Zhao Y, Li X, Li W, Zhao L, Li J, Ren Y, Xu Y. HPV16 E6 oncoprotein-induced

upregulation of lncRNA GABPB1-AS1 facilitates cervical cancer progression by regulating miR-519e-5p/Notch2 axis. FASEB J. 2020; 34:13211–23. https://doi.org/10.1096/fj.202000762R PMID:32844486

50. Panda AC, Gorospe M. Detection and Analysis of Circular RNAs by RT-PCR. Bio Protoc. 2018; 8:e2775. https://doi.org/10.21769/BioProtoc.2775 PMID:29644261

51. Mao S, Zhang S, Zhou S, Huang T, Feng W, Gu X, Yu B. A Schwann cell-enriched circular RNA circ-Ankib1 regulates Schwann cell proliferation following peripheral nerve injury. FASEB J. 2019; 33:12409–24. https://doi.org/10.1096/fj.201900965R PMID:31415184

SUPPLEMENTARY MATERIALS

Supplementary Figures

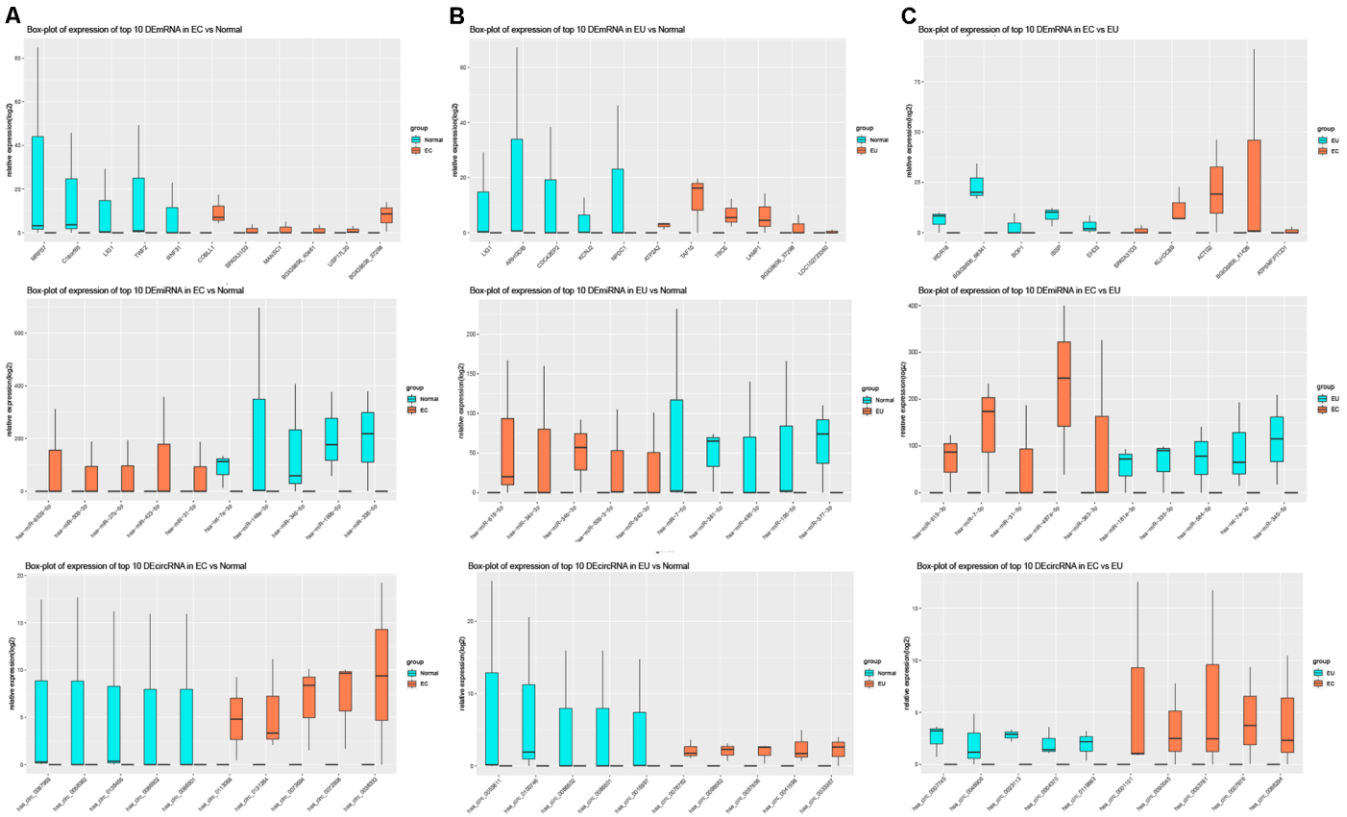

Supplementary Figure 1. Histogram showing the expression of the top 10 DECs, DEMis and DEMs between the EC and Ctrl (**A**), EU and Ctrl (**B**) and EC and EU groups (**C**).

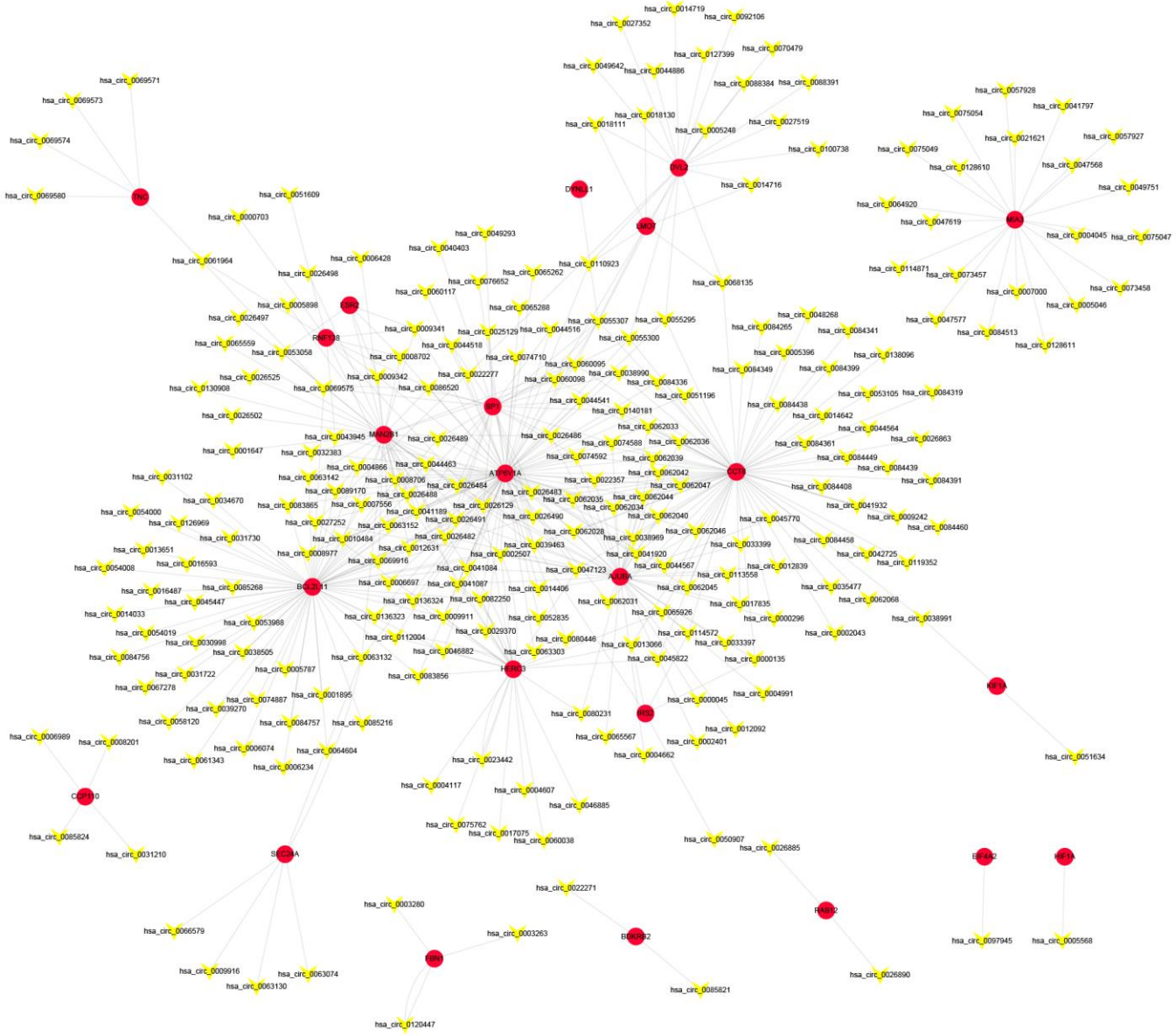

Supplementary Figure 2. The circRNA-mRNA co-expression network. Yellow V-shaped nodes represent DECs, and red circular nodes represent DEMs.

Supplementary Tables

Supplementary Table 1. GSEA of the DEMs in three comparison sets.

GROUP	NAME	NG*	NES	NOM p-val	FDR q-val
EC vs. Ctrl	**GO_POST_GOLGI_VESICLE_MEDIATED_TRANSPORT**	**79**	**2.13**	**0**	**0.0338**
	GO_REGULATION_OF_CARDIAC_CONDUCTION	53	2.103	0	0.0266
	GO_REGULATION_OF_P38MAPK_CASCADE	22	2.091	0	0.0205
	GO_NEGATIVE_REGULATION_OF_STRESS_ACTIVATED_PROTEIN_KINASE_SIGNALING_CASCADE	39	2.049	0	0.0356
	GO_MODULATION_BY_SYMBIONT_OF_HOST_CELLULAR_PROCESS	26	2.04	0.001	0.0344
	KEGG_VASCULAR_SMOOTH_MUSCLE_CONTRACTION	99	1.791	0	0.2194
	KEGG_UBIQUITIN_MEDIATED_PROTEOLYSIS	**132**	**1.77**	**0**	**0.1554**
	KEGG_PROTEASOME	42	1.764	0.001	0.1068
	KEGG_ALZHEIMERS_DISEASE	144	1.747	0	0.0939
	KEGG_CYSTEINE_AND_METHIONINE_METABOLISM	32	1.732	0.01	0.0907
EU vs. Ctrl	GO_POSITIVE_REGULATION_OF_DNA_TEMPLATED_TRANSCRIPTION_INITIATION	21	2.156	0	0.0362
	GO_REGULATION_OF_TRANSCRIPTION_INITIATION_FROM_RNA_POLYMERASE_II_PROMOTER	20	2.111	0	0.042
	GO_HYDROGEN_ION_TRANSMEMBRANE_TRANSPORT	**89**	**2.1**	**0**	**0.0345**
	GO_REGULATION_OF_DNA_TEMPLATED_TRANSCRIPTION_INITIATION	28	2.079	0	0.035
	GO_SNRNA_METABOLIC_PROCESS	78	2	0	0.0956
	KEGG_OXIDATIVE_PHOSPHORYLATION	**107**	**2.25**	**0**	**0**
	KEGG_BASAL_TRANSCRIPTION_FACTORS	33	1.92	0	0.0385
	KEGG_HUNTINGTONS_DISEASE	160	1.886	0	0.0343
	KEGG_PROTEASOME	41	1.871	0	0.0319
	KEGG_PARKINSONS_DISEASE	107	1.855	0	0.032
EC vs. EU	GO_CEREBELLAR_CORTEX_MORPHOGENESIS	28	2.229	0	0.0176
	GO_ADHERENS_JUNCTION_ORGANIZATION	**64**	**2.1**	**0**	**0.0743**
	GO_POSITIVE_REGULATION_OF_VIRAL_GENOME_REPLICATION	30	2.08	0	0.0624
	GO_MACROPHAGE_ACTIVATION	24	2.062	0.001	0.0559
	GO_RESPONSE_TO_DIETARY_EXCESS	16	2.055	0	0.0484
	KEGG_VASCULAR_SMOOTH_MUSCLE_CONTRACTION	115	1.791	0	0.2194
	KEGG_UBIQUITIN_MEDIATED_PROTEOLYSIS	**135**	**1.77**	**0**	**0.1554**
	KEGG_PROTEASOME	44	1.764	0.001	0.1068
	KEGG_ALZHEIMERS_DISEASE	157	1.747	0	0.0939
	KEGG_CYSTEINE_AND_METHIONINE_METABOLISM	34	1.732	0.01	0.0907

Note: The 6 most common gene sets were highlighted in table. GSEA: Gene Set Enrichment Analysis. DEMs: Differentially expressed mRNAs. Three comparison sets: EC vs. EU, EU vs. Ctrl and EC vs. EU. Ctrl: exosomes secreted by stromal cells of normal endometria from patient without endometriosis. EC: exosomes secreted by stromal cells of ovarian endometriomas from patient with endometriosis. EU: exosomes secreted by stromal cells of eutopic endometria from patient with endometriosis.

Supplementary Table 2. The top enriched GO BP terms and KEGG pathway terms of upregulated DEMs.

GO term	GO term description	GO term level 1	GO term level 2	Term gene num	Total gene num	P value
GO:0001837	epithelial to mesenchymal transition	biological_process	developmental process	51	24363	9E-05
GO:0010950	positive regulation of endopeptidase activity	biological_process	regulation of biological process	16	24363	3E-04
GO:2000562	negative regulation of CD4-positive, alpha-beta T cell proliferation	biological_process	biological adhesion	7	24363	3E-04
GO:0043687	post-translational protein modification	biological_process	metabolic process	438	24363	4E-04
GO:1902443	negative regulation of ripoptosome assembly involved in necroptotic process	biological_process	regulation of biological process	2	24363	4E-04
GO:0002062	chondrocyte differentiation	biological_process	developmental process	53	24363	8E-04
GO:0030177	positive regulation of Wnt signaling pathway	biological_process	regulation of biological process	53	24363	8E-04
GO:0010718	positive regulation of epithelial to mesenchymal transition	biological_process	developmental process	56	24363	0.001
GO:0032922	circadian regulation of gene expression	biological_process	metabolic process	78	24363	0.001
GO:0032774	RNA biosynthetic process	biological_process	metabolic process	3	24363	0.001
GO:1905426	positive regulation of Wnt-mediated midbrain dopaminergic neuron differentiation	biological_process	developmental process	3	24363	0.001
GO:0042698	ovulation cycle	biological_process	reproduction	11	24363	0.001
GO:1990253	cellular response to leucine starvation	biological_process	response to stimulus	11	24363	0.001
GO:0008286	insulin receptor signaling pathway	biological_process	regulation of biological process	104	24363	0.002
GO:0043123	positive regulation of I-kappaB kinase/NF-kappaB signaling	biological_process	regulation of biological process	239	24363	0.002
GO:0140052	cellular response to oxidised low-density lipoprotein particle stimulus	biological_process	response to stimulus	12	24363	0.002
GO:0038061	NIK/NF-kappaB signaling	biological_process	regulation of biological process	26	24363	0.002
GO:0043488	regulation of mRNA stability	biological_process	metabolic process	109	24363	0.002
GO:0006468	protein phosphorylation	biological_process	metabolic process	850	24363	0.002
GO:1903955	positive regulation of protein targeting to mitochondrion	biological_process	regulation of biological process	45	24363	0.002

KEGG pathway term	KEGG pathway term description	KEGG pathway term level 1	KEGG pathway term level 2	Term gene num	Total gene num	P value
410	beta-Alanine metabolism	Metabolism	Metabolism of other amino acids	42	15870	0.001
1100	Metabolic pathways	Metabolism	Global and overview maps	1923	15870	0.001
71	Fatty acid degradation	Metabolism	Lipid metabolism	57	15870	0.002
280	Valine, leucine and isoleucine degradation	Metabolism	Amino acid metabolism	64	15870	0.003
1130	Biosynthesis of antibiotics	Metabolism	Global and overview maps	327	15870	0.004
900	Terpenoid backbone biosynthesis	Metabolism	Metabolism of terpenoids and polyketides	34	15870	0.011
4013	MAPK signaling pathway	Environmental Information Processing	Signal transduction	103	15870	0.013
940	Phenylpropanoid biosynthesis	Metabolism	Biosynthesis of other secondary metabolites	3	15870	0.014
4072	Phospholipase D signaling pathway	Environmental Information Processing	Signal transduction	197	15870	0.014
4910	Insulin signaling pathway	Organismal Systems	Endocrine system	197	15870	0.014
4912	GnRH signaling pathway	Organismal Systems	Endocrine system	118	15870	0.018
4022	cGMP-PKG signaling pathway	Environmental Information	Signal transduction	228	15870	0.023

		Processing				
4062	Chemokine signaling pathway	Organismal Systems	Immune system	252	15870	0.031
5110	Vibrio cholerae infection	Human Diseases	Infectious diseases: Bacterial	62	15870	0.035
1212	Fatty acid metabolism	Metabolism	Global and overview maps	69	15870	0.042
4926	Relaxin signaling pathway	Organismal Systems	Endocrine system	164	15870	0.043
1110	Biosynthesis of secondary metabolites	Metabolism	Global and overview maps	558	15870	0.048
4152	AMPK signaling pathway	Environmental Information Processing	Signal transduction	175	15870	0.05

Note: GO BP: Gene ontology analysis of biological process. KEGG: Kyoto Encyclopedia of Genes. DEM: differentially expressed mRNA among the three comparison sets (EC vs. EU, EU vs. Ctrl, EC vs. EU).

Supplementary Table 3. The top enriched GO BP terms and KEGG pathway terms of downregulated DEMs.

GO term	GO term description	GO term level 1	GO term level 2	Term gene num	Total gene num	P value
GO:0006210	thymine catabolic process	biological_process	metabolic process	4	24363	1E-04
GO:0061179	negative regulation of insulin secretion involved in cellular response to glucose stimulus	biological_process	regulation of biological process	10	24363	0.001
GO:0001819	positive regulation of cytokine production	biological_process	regulation of biological process	41	24363	0.001
GO:0048643	positive regulation of skeletal muscle tissue development	biological_process	developmental process	15	24363	0.003
GO:0042445	hormone metabolic process	biological_process	metabolic process	18	24363	0.004
GO:0046475	glycerophospholipid catabolic process	biological_process	metabolic process	19	24363	0.004
GO:0035518	histone H2A monoubiquitination	biological_process	metabolic process	20	24363	0.005
GO:0090557	establishment of endothelial intestinal barrier	biological_process	developmental process	21	24363	0.005
GO:0000415	negative regulation of histone H3-K36 methylation	biological_process	metabolic process	1	24363	0.005
GO:0002731	negative regulation of dendritic cell cytokine production	biological_process	regulation of biological process	1	24363	0.005
GO:0006743	ubiquinone metabolic process	biological_process	metabolic process	1	24363	0.005
GO:0019859	thymine metabolic process	biological_process	metabolic process	1	24363	0.005
GO:0034143	regulation of toll-like receptor 4 signaling pathway	biological_process	immune system process	1	24363	0.005
GO:0034213	quinolinate catabolic process	biological_process	metabolic process	1	24363	0.005
GO:0036138	peptidyl-histidine hydroxylation	biological_process	metabolic process	1	24363	0.005
GO:0042265	peptidyl-asparagine hydroxylation	biological_process	metabolic process	1	24363	0.005
GO:0042790	nucleolar large rRNA transcription by RNA polymerase I	biological_process	metabolic process	1	24363	0.005
GO:0045221	negative regulation of FasL biosynthetic process	biological_process	metabolic process	1	24363	0.005
GO:0071166	ribonucleoprotein complex localization	biological_process	localization	1	24363	0.005
GO:0071881	adenylate cyclase-inhibiting adrenergic receptor signaling pathway	biological_process	signaling	1	24363	0.005
KEGG pathway term	**KEGG pathway term description**	**KEGG pathway term level 1**	**KEGG pathway term level 2**	**Term gene num**	**Total gene num**	**P value**
410	beta-Alanine metabolism	Metabolism	Metabolism of other amino acids	42	15870	0.001
1100	Metabolic pathways	Metabolism	Global and overview maps	1923	15870	0.001
71	Fatty acid degradation	Metabolism	Lipid metabolism	57	15870	0.002

280	Valine, leucine and isoleucine degradation	Metabolism	Amino acid metabolism	64	15870	0.003
1130	Biosynthesis of antibiotics	Metabolism	Global and overview maps	327	15870	0.004
900	Terpenoid backbone biosynthesis	Metabolism	Metabolism of terpenoids and polyketides	34	15870	0.011
4013	MAPK signaling pathway - fly	Environmental Information Processing	Signal transduction	103	15870	0.013
940	Phenylpropanoid biosynthesis	Metabolism	Biosynthesis of other secondary metabolites	3	15870	0.014
4072	Phospholipase D signaling pathway	Environmental Information Processing	Signal transduction	197	15870	0.014
4910	Insulin signaling pathway	Organismal Systems	Endocrine system	197	15870	0.014
4912	GnRH signaling pathway	Organismal Systems	Endocrine system	118	15870	0.018
4022	cGMP-PKG signaling pathway	Environmental Information Processing	Signal transduction	228	15870	0.023
4062	Chemokine signaling pathway	Organismal Systems	Immune system	252	15870	0.031
5110	Vibrio cholerae infection	Human Diseases	Infectious diseases: Bacterial	62	15870	0.035
1212	Fatty acid metabolism	Metabolism	Global and overview maps	69	15870	0.042
4926	Relaxin signaling pathway	Organismal Systems	Endocrine system	164	15870	0.043
1110	Biosynthesis of secondary metabolites	Metabolism	Global and overview maps	558	15870	0.048
4152	AMPK signaling pathway	Environmental Information Processing	Signal transduction	175	15870	0.05

Supplementary Table 4. Primers used in this study.

Names	Sequences(5'-3')
hsa-miR-15a-5p	Forward: GGGTCGTAGCAGCACATAATGG
hsa-circ_0026129	Forward: AAGTATTCCCTGTCTTAAGCCGAC
	Reverse: CTTGCCATAATCAACTGAGAGACG
ATP6V1A	Forward: ACAGCCTCTGGGTCCTCGGTCG
	Reverse: CCTGAGACCCCATGCACATAACCAA
U6	Forward: CTCGCTTCGGCAGCACA
	Reverse: AACGCTTCACGAATTTGCGT
GAPDH	Forward: ACAGCCTCAAGATCATCAGC
	Reverse: GGTCATGAGTCCTTCCACGAT